Indian Journal of Fibre & Textile Research
Vol. 46, June 2021, pp. 144-148

Preparation and properties of PVA/SS/AgNPs composite nanofibres

Zhang Xianhua[a], Yun Fucheng & Yuan Mingzhong

School of Textiles, Henan University of Engineering, Zhengzhou 450007, China

Received 1 November 2019; revised received and accepted 20 November 2020

Polyvinyl alcohol (PVA), PVA/silk sericin (SS) and PVA/SS/AgNPs (nano-silver) solutions have been prepared, and the nanofibres are produced by electrospinning technology. The nanofibres are then tested using scanning electron microscopy (SEM), Fourier transform infrared spectroscopy (FTIR) and X-ray diffraction (XRD). The results show that the morphology of 7-11 wt% PVA nanofibres is fine and smooth. With the increase in SS and AgNPs contents, the average diameter of PVA/SS and PVA/SS/AgNPs composite nanofibres is increased. The FTIR spectra and XRD patterns of PVA/SS/AgNPs composite nanofibres with different mass ratios have the similar regular curves. The intensity of the infrared peak of PVA/SS/AgNPs composite nanofibres weakens at 837, 1087, 1648 and 2914 cm^{-1} with the increase in AgNPs; the intensity of the diffraction peak gradually increases at 13.1° and weakens at 19.09 °. This may be due to the reason that Ag interacts with PVA and SS molecules. The findings are of great significance for the development of nano-scale antibacterial fibres.

Keywords: Antibacterial fibres, Electrospinning, Nanofibres, Nano-silver, Polyvinyl alcohol, PVA/SS/AgNPs Composite, Sericin

1 Introduction

Electrospinning is a technique for preparing nanofibres by moving and deflecting the charged solution which is ejected onto the aluminum foil receiver under the electric field force[1,2]. A certain amount of solution is sucked using a syringe. As the voltage continuously increases and the spinning pump is pushed, the solution in the syringe is bound away from the surface tension, and nanofibres are formed on the aluminum foil receiver through the spinneret due to the evaporation of the solution[3-6]. Nanofibres have a controlled fibre thickness, a large specific surface area, and interconnected porous structures[7,8].

Polyvinyl alcohol (PVA) is non-toxic and biodegradable[9-11], which has good stability and can improve the spinnability. It does not volatilize harmful substances during the electrospinning process using water as the solvent[12,13]. Silk sericin (SS) is a silk protein secreted by silkworm[14], which contains a large number of hydrophilic amino acids[15-17], and is widely used in the field of cosmetics[18-20]. However, the membrane prepared directly from pure SS is easily soluble in water and has poor mechanical properties. In order to make full use of the functional properties, SS and other polymers are typically mixed or crosslinked[21-23] to form new materials for use.

AgNPs refer to tiny silver particles with the size between 1 nm and 100 nm. It has the characteristics of large specific surface area, small size effect, quantum effect and so on. It is known for its unique optical, electrical, thermal and magnetic properties[24-27]. Compared to conventional size silver particles, its chemical and biological activities are significantly enhanced[28,29]. AgNPs have high catalytic activity, strong adsorption capacity, controllable diameter and high antibacterial activity[30-32]. Generally, the strong antibacterial property is determined by small particle size, high valence state, large specific surface area and low solution concentration. It is widely used in cosmetics, medicine, food packaging materials and other fields[33-37]. At present, the preparation of functional composites based on AgNPs has become a research hotspot.

In this study, PVA, PVA/SS and PVA/SS/AgNPs solutions have been prepared using deionized water (H_2O) as the solvent, and nanofibre materials are fabricated by electrospinning technology. In order to select the optimal mass ratio of the PVA/SS/AgNPs composite nanofibres, the effect of different content of AgNPs on the conformation of composite nanofibres is investigated, which is beneficial to develop nano-antibacterial products in the future. The properties of the nanofibre materials are then investigated using SEM, FTIR and XRD.

[a]Corresponding author.
E-mail: Xianhuaz@haue.edu.cn

2 Materials and Methods

2.1 Materials

Sericin (SS) was procured from Favorsun Pharmaceutical Co., Ltd, Shanghai; PVA1797 (Alcoholysis degree 96.0-98.0%) from Aladdin Industrial Corporation; deionized water from Zhengzhou Erqi District Changhe Distilled Water Sales Department; and AgNPs(60-120 nm) from Aladdin Industrial Corporation.

2.2 Experimental Instruments

UX620H electronic balance (SYU3-100D ultrasonic), constant temperature water bath with magnetic stirrer (DF-101S), LSP01-1A Lange syringe pump and D-ES50PN-10W/DDPM electrostatic high-voltage generator were used.

2.3 Preparation of Electrospinning Solution

2.3.1 PVA Solution

Different amount of PVA (3, 5, 7, 8, 9 and 11g) and deionized water (97, 95, 93, 92, 91 and 89g) were separately added into the blue cap bottle, and allowed to swell for 1 h at room temperature (25ºC). A uniform transparent PVA solution was obtained after stirring at 95 °C for 4 h.

2.3.2 PVA/SS Solution

Four parts of 8g PVA (as in section **2.3.1**) were weighed, and added into 91,90,89 and 87g of deionized water individually, to which 1,2,3 and 5g of SS was added respectively. The PVA/SS blend solution was prepared at 60°C for 2h in the water bath.

2.3.3 PVA/SS/AgNPs Solution

Deionized water (89.98, 89.97, 89.96, 89.95 and 89.94 g) was added to AgNPs (0.02, 0.03, 0.04, 0.05 and 0.06 g), which is then dispersed using ultrasound for 45 min and stirred in the constant temperature water bath with magnetic stirrer for 30 min. To prepare PVA/SS/AgNPs solution, five parts of 8g PVA and 2g SS (as in section **2.3.2**) were weighed and poured into AgNPs solutions respectively.

2.4 Preparation of Nanofibre Membrane

The 5 mL spinning solution was taken in the syringe which was installed on the syringe pump and air was expelled while filling the syringe. An aluminum foil paper was attached on the receiving device. The conditions used for spinning were distance 12cm, voltage 16kV and spinning speed 0.35mL/h for PVA solution, 1.2mL/h for PVA/SS solution and 1.5mL/h for PVA/SS/AgNPs solution respectively.

2.5 Electron Microscopy

The nanofibre samples were placed on the sample stage and sprayed with gold for 30 s in the vacuum coating machine and scanned using the ZEISS Sigma 500 (Germany) scanning electron microscope. Diameters of 100 fibres were measured using Image J in the electron micrograph, then the average diameter and the standard deviation were calculated.

2.6 Infrared Spectroscopy

The total reflection infrared spectra of PVA/SS/AgNPs nanofibres was measured using thermo Fisher Nicolet 6700 Fourier transform infrared spectroscopy (FTIR)with wavenumber range of 250-4500 cm^{-1} and resolution of 0.09 cm^{-1}.

2.7 X-Ray Diffraction

The X-ray diffraction was measured by the D8 ADVANCE X-ray diffractometer with a CuKα source ($\lambda = 1.5418$) and the operating voltage is 40 kV and the current was 30 mA. The scanning speed was 2 °/min and the angle range is 10-80 °.

3 Results and Discussion

3.1 Electron Microscope Photograph of PVA Nanofibres

Figure 1(a) shows that 3 wt% PVA nanofibres have curvature, irregular triangular structure, bead string structure, a small amount of spindle structure and a small amount of irregular polygonal structure with large area. The morphology of the fibres varies greatly and the thickness of the fibres is uneven. It can be seen from Fig. 1(b) that when the PVA is 5 wt%, there are a few thin nanofibres, a large number of spindle structures and a small number of beads. The unevenness between the fibres is high. Figure 1(c) shows that when PVA is 7 wt%, there are very few spindle structure and many fibres bonding in nanofibres. The diameter of 7 wt% PVA nanofibres is more uniform than those of 3 wt% and 5 wt% PVA nanofibres. Figures 1(d), (e) and (f) show that 8wt% PVA nanofibres is the thinnest. The diameters of 9 wt% and 11 wt% PVA nanofibres are relatively uniform. There are no obvious irregular structure or bonding phenomenon and the spinning effect is good.

In order to study the difference of PVA nanofibres with different concentration deeply, the diameter of nanofibres is measured by Image J and the average diameter and standard deviation of 100 nanofibres are calculated using Excel. The average diameters (standard deviation) for 7, 8, 9 and 11 wt PVA nanofibres are 146.7nm (30.4), 135.3nm (35.3), 349.1nm (57.2) and 315.6nm (64.9) respectively.

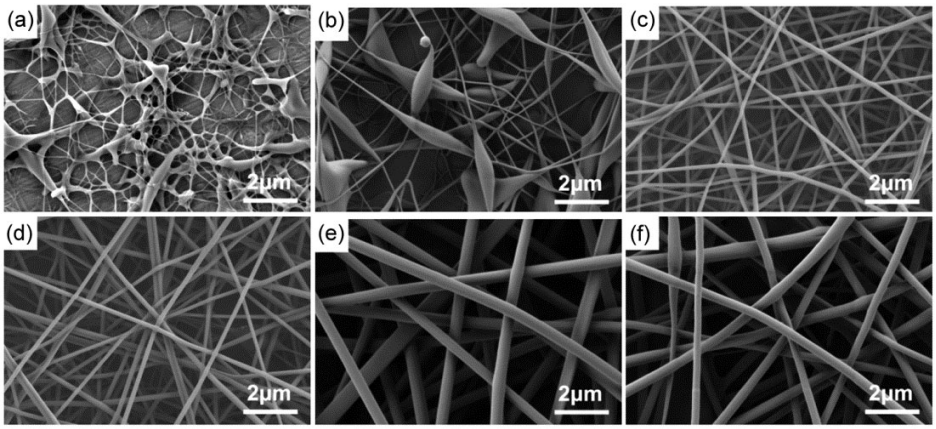

Fig. 1—Electron micrograph of PVA nanofibres (a) 3 wt%; (b) 5 wt%; (c) 7 wt%; (d)8 wt%; (e)9 wt% and (f)11 wt%

It can be seen that the average and standard deviation of the fibre diameters of 7 wt%, and 8 wt% PVA nanofibres are not significantly different, but their average diameters are obviously smaller than that of 9 and 11 wt% PVA nanofibres. The uniformity and morphology of the fibres are significantly better than those of 9 wt% and 11 wt% PVA nanofibres. When the experimental materials and conditions are the same, the diameter of 8 wt% PVA nanofibres is the smallest and the morphology is relatively good.

3.2 Electron Microscope Photograph of PVA/SS Composite Nanofibres

Figure 2(a) shows that the nanofibres have the bonding phenomenon andthe surface of the nanofibresis rough, concave and convex when the PVA/SS is 8:1. The thickness of the nanofibres is not uniform. The PVA/SS (8:2, 8:3 and 8:5) composite nanofibres have adhesions in varying degrees [Figs 2(b)-(d)]. In a further study of the PVA/SS composite nanofibres, the average diameters (standard deviation) for 8:1, 8:2, 8:3 and 8:5 PVA/SS mass ratios are 433.6nm (62.8), 450.6nm (98.5), 454.7nm (78.9), and 491.3 nm (86.6) respectively.

The average diameter of the nanofibres with different mass ratios increases with the increase of SS content. The diameter standard deviation could be used to judge that the uniformity of PVA/SS (8:1) is the best and PVA/SS (8:2) is the worst. However, PVA/SS (8:1) nanofibres have an obvious fibre bonding phenomenon. Under the same experimental conditions, PVA/SS (8:3) composite nanofibres is the best mass ratio.

3.3 Electron Microscope Photograph of PVA/SS/AgNPs Composite Nanofibres

In order to study the effect of different content of AgNPs on the appearance of PVA/SS/AgNPs composite nanofibres, the surface morphology of PVA/SS/AgNPs composite nanofibres is studied by electron microscopy. The results are shown in Fig. 3.

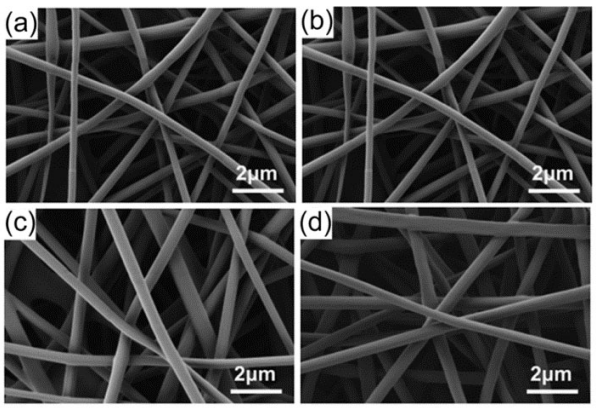

Fig. 2—Electron microscope photographs of PVA/SS composite nanofibres with different mass ratios (a) 8:1, (b) 8:2, (c) 8:3 and (d) 8:5

It can be seen from Fig. 3(a) that PVA/SS/AgNPs (8:2:0.02) composite nanofibres have smooth surface, no bead phenomenon and uniform diameter distribution. With the increase of the mass fraction of AgNPs [Figs 3(b)-(e)], the diameter of the fibres increases, and the adhesion between the nanofibres also occurs. In order to further study the influence of AgNPs content on the diameter of composite nanofibres (PVA/SS/AgNPs), the average diameter (standard deviation) of 100 nanofibres for 8:2:0.02, 8:2:0.03, 8:2:0.04, 8:2:0.05 and 8:2:0.06 PVA:SS: AgNPs mass ratios are 149.7nm (5.9), 308.4nm (9.5), 368.1nm (11.5), 378.7nm (13.0) and 389.2nm (12.7) respectively.

The average diameter of PVA/SS/AgNPs composite nanofibres increases from 149.7 nm to 389.2 nm with the increase in AgNPs, when other

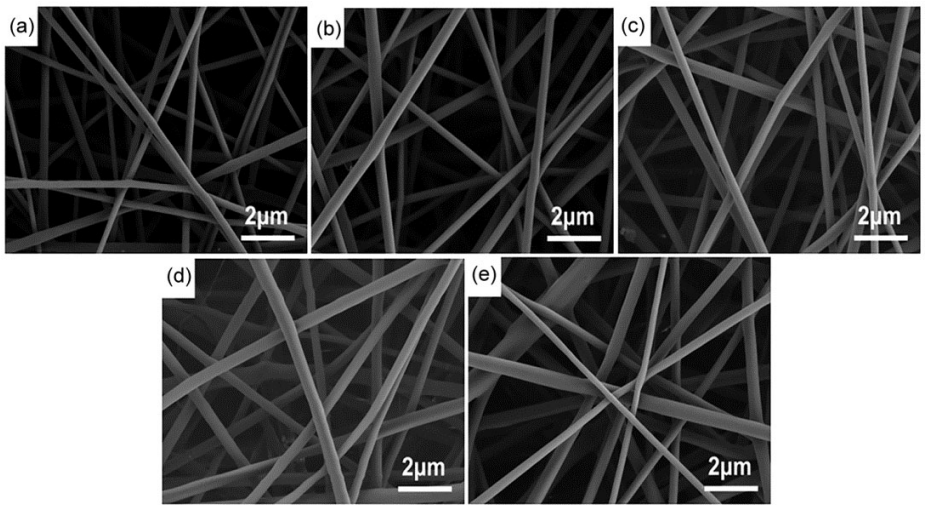

Fig. 3—PVA/SS/AgNPs composite nanofibres with different mass ratios (a) 8:2:0.02; (b) 8:2:0.03; (c) 8:2:0.04; (d) 8:2:0.05 and (e) 8:2:0.06

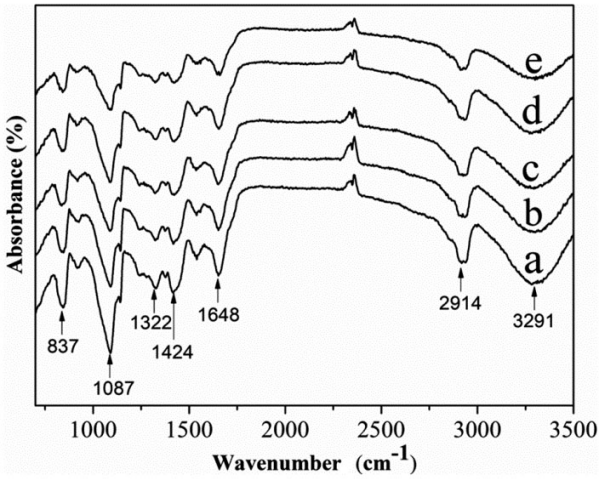

Fig. 4—Infrared spectra of PVA/SS/AgNPs composite nanofibres with different mass ratios (a)8:2:0.02, (b) 8:2:0.03, (c) 8:2:0.04, (d) 8:2:0.05 and (e) 8:2:0.06

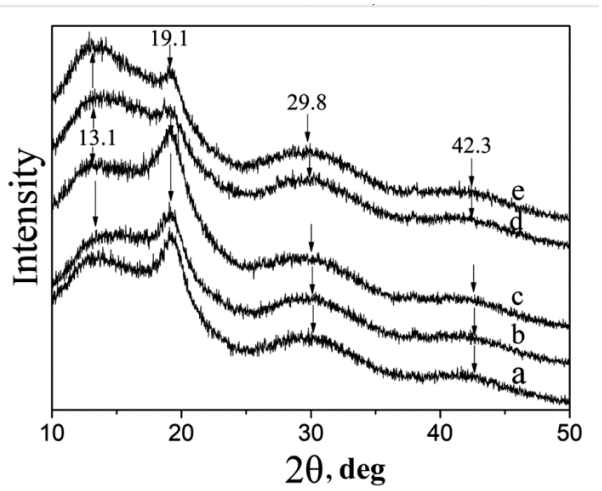

Fig. 5—X-ray diffraction patterns of PVA/SS/AgNPs composite nanofibres with different mass ratios (a) 8:2:0.02, (b) 8:2:0.03, (c) 8:2:0.04, (d) 8:2:0.05 and (e) 8:2:0.06

conditions are fixed in the process of preparing nanofibres. The standard deviation of fibre diameter gradually increases and it tends to be stable after increasing to a certain extent. This maybe because that the conductivity of the PVA/SS/AgNPs solution increases because of the increasing content of AgNPs. Under these experimental conditions, the average diameter and diameter standard deviation PVA/SS/AgNPs (8:2:0.02) are smallest.

3.4 Infrared Spectra of PVA/SS/AgNPs Composite Nanofibres

The infrared spectra of PVA/SS/AgNPs composite nanofibres are analyzed by FTIR (Fig. 4).

The curves of the infrared absorption spectra of PVA/SS/AgNPs composite nanofibres with different mass ratios are similar and the peak values are 837, 1087, 1322, 1424, 1648, 2914 and 3291 cm^{-1} (Fig. 4). The intensity of the peak decreases with the increase of AgNPs at 837, 1087, 1648 and 2914 cm^{-1}, which may be due to the interaction of Ag with PVA or SS molecules.

3.5 X-ray Diffraction of PVA/SS/AgNPs Composite Nanofibres

The changes in the crystalline structures of PVA/SS/AgNPs composite nanofibres, were analysed using X-ray diffraction. The results are shown in Fig. 5.

The X-ray diffraction patterns of PVA/SS/AgNPs composite nanofibres with different mass ratios are found to be similar (Fig. 5). The peaks of the X-ray

diffraction are 13.1, 19.1, 29.8 and 42.3 °. With the increase of AgNPs, the intensity of the diffraction peaks of PVA/SS/AgNPs composite nanofibres increases gradually at 13.1 ° and weakens at 19.09 °. The reason may be that Ag interacts with PVA and SS molecules.

4 Conclusion

The PVA, PVA/SS and PVA/SS/AgNPs nanofibres have been fabricated by electrospinning using deionized water as solvent. Under these experimental conditions, 8 wt% PVA nanofibres have the best morphology; with the increase of SS content, the average diameter of PVA/SS composite nanofibres increases. With the increase of AgNPs content, the average diameter of PVA/SS/AgNPs composite nanofibres increases. The infrared absorption spectra and X-ray diffraction patterns of PVA/SS/AgNPs composite nanofibres with different mass ratios are found to be similar. The infrared peaks are 837, 1087, 1322, 1424, 1648, 2914 and 3291 cm^{-1} and the intensity of the peaks decreases with the increase of AgNPs at 837, 1087, 1648 and 2914 cm^{-1}.The peaks of the diffraction patterns are 13.1, 19.1, 29.8 and 42.3° respectively. With the increasing content of AgNPs, the intensity of the diffraction peaks of PVA/SS/AgNPs composite nanofibres increases gradually at 13.1°, and weakens at 19.09^{o}. The reason may be that Ag interacts with PVA and SS molecules. The results are of great significance for the development of antibacterial nanofibres.

Acknowledgement

The authors gratefully acknowledge the funding support by Henan University of Engineering (Doctoral fund project D2017005).

References

1 Dharmansh D & Paresh C, *Polymer*, 131(2017)34.
2 Weiguang S, Dagang L, Nana P & Renjie S, *Macromolecules*,18(2017)3273.
3 Jianghui Z, Xiaoxia L & Zhi L, *J Low Frequency Noise, Vibration Active Control*, 38(3-4)(2019) 1338.
4 Rouxi C, Yuke W, Jie F, Liang W, Zhibo S, Liming Q, Libing L, Yantao L, Jianhua C & Yong L, *J Low Frequency Noise, Vibration Active Control*, 38(3-4)(2019)1687.
5 Alexander RN, Cormac DF, Gordon GW, Zhigang X, Xungai W & Michael JH, *Nanotechnology*, 30 (2019)1.
6 Zhihu W, Hongwei H, Guosai L, Xu Y, Xin N & Yunze L, *Materials Letters*, 254(2019)5.
7 Jian Q, Tianshuai W, Dongye L, Enzuo L, Naiqin Z, Chunsheng S, Fang H, Liying M & Chunnian H, *Adv Mater*, 30(2018)1.
8 Haiyan D, Tingting Y, Guorong C, Jianping Z, Liyi Shi & Dengsong Z, *Chem Commun*, 53(2017)7465.
9 Purwar R, Sharma S, Sahoo P & Srivastava CM, *Fibres Polymers*,16(4)(2015)761.
10 Tao G, Wang Y, Cai R, Chang H, Song K, Zuo H, ZhaoP, Xia Q & He H, *Materials Sci Eng C*, 101(2019)341.
11 Mohammad FA, Fatemeh N, Navid N, Zahra ASK, Bahareh N, Seyed EE & Hassan M, *Gene*, 720(2019)1.
12 Huafeng T, Yuan L, Jianguo W, Hao W & Hailiang W, *J Hazardous Materials*, 378(2019)1.
13 Akikazu S, Hayato K, Taiga S & Masahito K, *Japanese J Appl Phys*,56 (2017)1.
14 Yun H, Kim MK, Kwak HW , Lee JY & Lee KH, *Fibres Polym*, 14(12)(2013)2111.
15 Züge LCB, Silva VR, Hamerski F, Ribani M, Gimenes ML & Scheer AP, *J Food Process Eng*, 40(1)(2015)1.
16 Nishida A, Yamada M, Kanazawa T, Takashima Y, Ouchi K & Okada H, *Int J Pharmaceutics*, 407(1-2)(2011)44.
17 Oh H, Ji YL, Kim MK, Um I C & Lee KH, *Int J Biol Macromol*, 48(1)(2011)32.
18 Kim SJ & Um IC, *Fibres Polym*, 20(2)(2019)271.
19 Jang MJ & Um IC, *Eur Polym J*, 20(2)(2017)761.
20 Inês KR, Costa BRM, Chasko RLDF & Maral NMR, *BioMed Res Int*, 2016(2016) 1.
21 Zhang HP, Wang XY, Min SJ, Mandal M, Yang MY & Zhu LJ, *Ceramics Int*, 40(1)(2014)985.
22 Ai L, Wang Y, Tao G, Zhao P, Umar A, Peng W & Huawei H, *Molecules*, 24(503)(2019)1.
23 Xianhua Z, Xiangwei F, Rong Z, Fan L, Chuang H & Jie W, *Digest J Nanomaterials Biostructures*,14(3)(2019)797.
24 Beyene HD, Werkneh AA, Bezabh HK & Ambaye TG, *Sustainable Materials Technol*, 13(2017)18.
25 Shi J, Xu B, Sun X, Ma C, Yu C & Zhang H, *Aquatic Toxicology*, 132-133(2013)53.
26 Butler KS, Peeler DJ, Casey BJ, Dair BJ & Elespuru RK, *Mutagenesis*, 30(4)(2015)577.
27 Bapat RA, Chaubal TV, Joshi CP, Bapat PR, Choudhury H, Pandey M, Gorain B & Kesharwani P, *Materials Sci Eng: C*, 91(2018)881.
28 Ragaa AH, Mervat HH, Rasha AA & Salwa SB, *Scientific Reports*, 9(2019):1.
29 Wang C, Huang X, Deng W, Chang C, Hang R & Tang B, *Materials Sci Eng: C*, 41(2014)134.
30 Rafieerad AR, Bushroa AR, Nasiri-Tabrizi B, Baradaran S, Amiri A, Saber-Samandari S, Khanahmadi S, Zeimaran E,Basirun WJ, Kalaiselvam K,Vellasamy KM & Vadivelu J, *Surface Coatings Technol*, 360(2019)181.
31 Ananthi V, Prakash GS, Rasu KM, Gangadevi K, Boobalan T, Raja R, Anand K, Sudhakar M, Chuturgoon A & Arun A, *J Photochem Photobiol, B: Biology*, 186(2018)232.
32 Li J, Liu X, Lu J, Wang Y, Li G & Zhao F, *J Colloid Interface Sci* , 484(2016)107.
33 You C, Han C, Wang X, Zheng Y, Li Q, Hu X & Sun H, *Molecular Biology Reports*, 39(2012)9193.
34 Murphy M, Ting K, Zhang X, Soo C & Zheng Z, *J Nanomaterials*, 2015(2015)1.
35 Beyene HD, Werkneh AA, Bezabh HK &A mbaye TG, *Sustainable Materials Technol*, 13(2017)18.
36 Carbone M, Donia DT, Sabbatella G & Antiochia R, *J King Saud University-Science*, 28(2016)273.
37 Mackevica A, Olsson ME & Hansen SF, *J Nanoparticle Res*, 18(5)(2016) 1.